

# Real-Time Robot Trajectory Estimation and 3D Map Construction using 3D Camera

Kazunori Ohno

GSIS, Tohoku University.

6-6-01 Aramaki Aza Aoba, Aoba-ku, Sendai  
 980-8579, JAPAN.

Email: kazunori@rm.is.tohoku.ac.jp

Takafumi Nomura

Terumo Corporation.

44-1,2-chome, Hatagaya,  
 Shibuya-ku, Tokyo,  
 151-0072, JAPAN

Satoshi Tadokoro

GSIS, Tohoku University.

6-6-01 Aramaki Aza Aoba, Aoba-ku, Sendai  
 980-8579, JAPAN.

Email: tadokoro@rm.is.tohoku.ac.jp

**Abstract**—Our research objective is Simultaneous Localization and Mapping (SLAM) in rubble environment. The map construction requires estimation of robot trajectory in 3D space. However, it is hard to estimate it by using odometry or gyro in rubble. In this paper, the authors proposed real-time SLAM based on 3D scan match. 3D camera is used for measurement of 3D shape and its texture in real-time. 3D map and robot trajectory are estimated by combining these 3D scan data. ICP algorithm is used for the matching method. The authors modified ICP algorithm as fast and robust one for real-time 3D map construction.

**Index Terms**—SLAM on Rubble, 3D camera, Fast and Robust ICP, Rescue Robot.

## I. INTRODUCTION

Research objective of the authors is 3D map building and localization for the snake-like rescue robot (Fig. 1). In this paper, the authors present our approach for the robot trajectory estimation and 3D map construction based on 3D shape matching method. ICP algorithm was used for the matching method. For real-time use, the authors improved its matching speed and analyzed its robustness.

Studies about rescue robots have been progressing rapidly after Hanshin-Awaji (Kobe) earthquake and multiple acts of terror in NY. In Japan, MEXT<sup>1</sup> Special Project for Earthquake Disaster Mitigation in Urban Areas Advanced Disaster Management System started in 2002. Main task of the rescue robot is information collection in a rubble environment. Especially, map construction is one of big issues. The authors have joined this project, and studied rescue robot localization and map building.

Recently, many researchers are interested in Simultaneous Localization and Mapping (SLAM) in unknown environment [1], [2], [3]. In SLAM, continuous robot motion and environment map were simultaneously estimated by fusion of odometry, gyro, LRF etc. Precise robot position and map were obtained by closing trajectory loop. Moreover, some researches proposed SLAM with detection and tracking of moving object [4], [5] and effective calculation method of SLAM [6], [7]. However, on rubble environment (e.g.

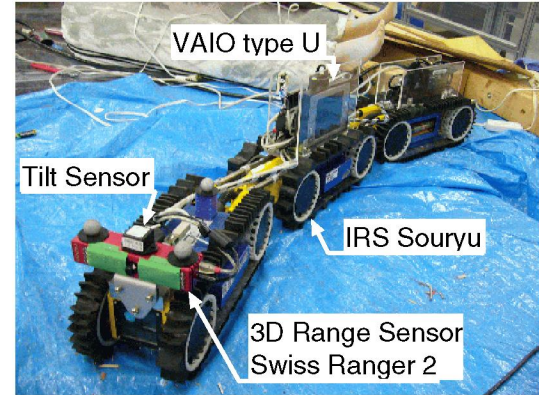


Fig. 1. Snake Type Robot "IRS Souryu"

earthquake, car accident, fire disaster area), it is hard to estimate continuous robot motion by using odometry or gyro. Especially, the snake-like robot is too difficult to model the robot's odometry for estimation of robot motion. Therefore, if SLAM framework is used for the robot localization and mapping, it is necessary to derive the robot motion without odometry.

The authors think that SLAM based on 3D shape matching method is one of good solutions for the problem on rubble. Nagatani proposed Sphere Digital Elevation Map (S-DEM) as a method of 3D shape match [8]. In this study, sparse crawler robot position and 3D map were estimated from 3D shapes. Following the research, the authors did the map building and the robot localization by matching the 3D shapes of the rubble.

In our proposed method, 3D shape is measured at small interval by using real-time 3D camera. Continuous robot trajectory and 3D map are estimated by matching these 3D shape. This method does not need precise robot's motion model in contrast to usual odometry based method. This advantage is important for searching rubble environment.

This method requires fast and robust matching method. ICP algorithm was selected as the matching one. ICP algorithm is useful for matching two scan data measured at

<sup>1</sup>Ministry of Education, Culture, Sports, Science and Technology

small motion, and frequently used in previous studies [9]. The authors improved ICP process speed keeping robustness.

In this paper, the authors propose a novel method for real-time 3D map construction in Sec. II. The specs for 3D camera are described in Sec. III. The authors developed fast and robust ICP algorithm for real-time 3D map construction and localization. The details of fast and robust ICP algorithm and its accuracy are explained in Sec. IV. To verify practicality of our method, the authors demonstrated offline experiments of 3D map construction in laboratory and collapsed house simulation facility. System which was used in experiments and results of experiments are illustrated in Sec. V. From these results, the authors conclude in Sec. VI.

## II. STRATEGY OF 3D MAP BUILDING

The authors aim to realize the 3D map construction and the localization combining 3D shapes measured at small interval. The authors used a 3D camera for the real-time measurement of 3D shape. Estimating continuous robot position requires a development of 3D scan matching in real time. ICP algorithm was used for the scan matching. The accuracy of ICP depends whether below assumptions are satisfied.

- Input data is almost the same as reference data if two data are measured at close viewpoint.
- The point corresponded to a point in the input data can be found as the nearest point in reference data when the motion between these scan data is small.

Our 3D shape measurement condition satisfies the above two assumptions of ICP algorithm. In this paper, the authors developed a fast and robust ICP algorithm for speedup of matching process.

Figure 2 illustrates the process flow of the 3D map construction.  $\mathbf{P}_t$  is a 3D shape measured by the 3D camera.  $(\phi, \theta)$  is the sensor's posture measured by an accelerometer.  $\phi$  and  $\theta$  present its roll and pitch respectively. Motion  $M_t = \{\mathbf{R}_t, \mathbf{t}_t\}$  is calculated from two adjoining scans  $\{\mathbf{P}_{t-1}, \mathbf{P}_t\}$ .  $\mathbf{R}_t = R(\theta)R(\psi)R(\phi)$  and  $\mathbf{t}_t = \{x, y, z\}$  represent rotation matrix and translation vector respectively. 3D map and continuous robot position are estimated by combining these motions  $M_t$  and these 3D shapes  $\mathbf{P}_t$ .

## III. 3D CAMERA

CSEM Swiss Ranger (SR-2), which can measure 3D shape  $\mathbf{P}_t$  and its texture  $\mathbf{G}_t$  in real time, was used in this approach (Fig.3)! This sensor's measurement principle is time-of-flight [12]. The camera is based on a 2-dimensional dedicated image sensor and a modulated light source. Every pixel on the sensor measures the amount of modulated light reflected by objects in the scene. The arrived time between object and each pixel is measured from this information. Then, distance between each pixel and the object  $d(u, v)$  is calculated from the arrived time. The gray-level (i.e., intensity) image  $\mathbf{G}_t$  is obtained simultaneously.

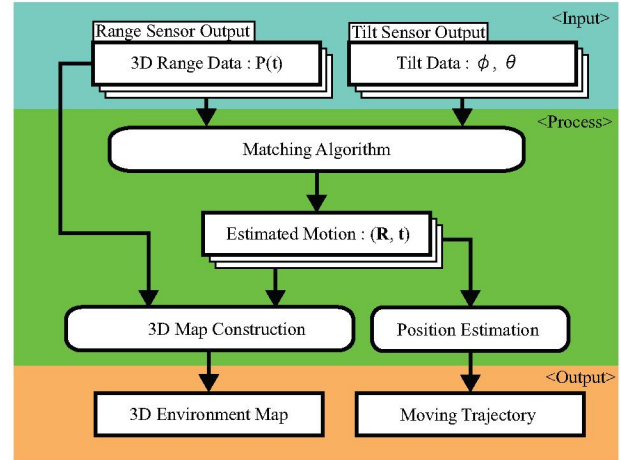


Fig. 2. Data Flow

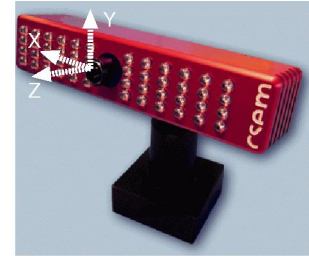


Fig. 3. Swiss Ranger SR-2

Table I shows the specification of the Swiss Ranger. This image sensor contains  $160 \times 124$  pixels. This sensor can measure distance of 19840 points  $d(u, v)$  at once. The authors defined it as pin-hole model and calculated 3D shape  $\mathbf{P}_t = \{p_1, p_2, \dots, p_N\} (N = 19840, p_i = (x, y, z))$  from  $d(u, v)$ . Let Z axis in the sensor coordinate be sensor's optical axis. X and Y are the horizontal direction of the image device and its vertical direction respectively (Fig. 3). Figure 4 illustrates a 3D shape measured by SR-2. Each pixel's color in the Fig. 4 varies from red to blue following Z value (far: blue, near: red). The authors measured its accuracy and plotted the result in Fig. 5. This sensor can not measure a distance within 50 [cm]. Measurement error increased over 350 [cm]. The authors only used data between 50 [cm] and 350 [cm] in this approach.

TABLE I  
TECHNICAL DATA FOR SWISS-RANGER SR-2

Number of Pixels	$124 \times 160$
Maximum Range	7.5 m
Frame Rate	Up to 30 fps
Field of View	42 ° x 46 °
Interface	USB 2.0
Lens	f= 8 mm
Dimensions	135 x 45 x 32 mm
Weight	200 g

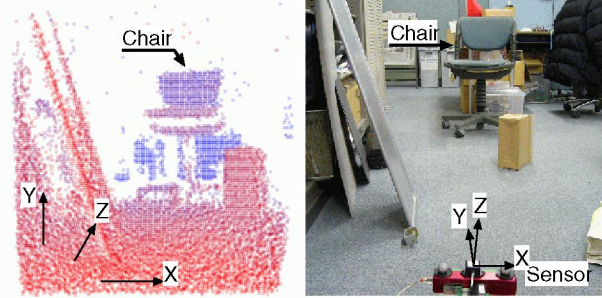


Fig. 4. Sample Measurement (In the Laboratory)

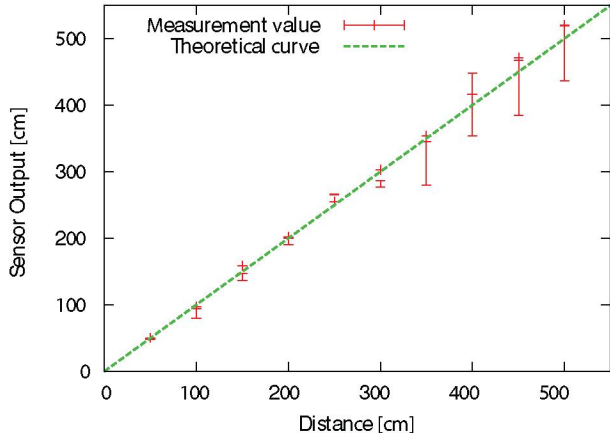


Fig. 5. Evaluation of Range Sensor Accuracy

#### IV. FAST AND ROBUST ICP ALGORITHM

##### A. Outline of ICP Algorithm

The objective of ICP algorithm is to find the motion  $M_t = \{R_t, t_t\}$  between two 3D shapes  $\mathbf{P}_{t-1}, \mathbf{P}_t$  measured by the 3D camera at different viewpoints. Details of the method were already explained in [10]. A pair of closest point in these two shape  $\mathbf{P}_{t-1}, \mathbf{P}_t$  is denoted as  $\{\mathbf{x}_i, \mathbf{y}_i\}$ .  $\mathbf{x}_i$  is a point of the input data  $\mathbf{P}_t$ .  $\mathbf{y}_i$  is a point of the reference data  $\mathbf{P}_{t-1}$ . The motion is derived by minimizing the following mean-squares objective function  $\mathcal{F}$  (Eq. 1).

$$\mathcal{F}(\mathbf{R}, \mathbf{t}) = \frac{1}{N} \sum_{i=1}^N \|\mathbf{R}\mathbf{x}_i + \mathbf{t} - \mathbf{y}_{j_{i-1}}\|^2 \quad (1)$$

where  $N$  is the number of pair (much greater than 3). ICP algorithm is a technique which derives the robot motion  $\mathbf{R}, \mathbf{t}$  and the pair of  $\mathbf{x}, \mathbf{y}$  by minimizing  $\mathcal{F}$ .  $\mathcal{F}$  is minimized by iteration of four steps as follows:

- Step 1, Finding matched point pair between input scan data  $\mathbf{P}_t$  and reference scan data  $\mathbf{P}_{t-1}$ .
- Step 2, Elimination of mismatched pair.
- Step 3, Estimation of motion.
- Step 4, Applying the estimated motion to  $\mathbf{P}_t$ .

These steps are iterated until the estimated motion converges.

TABLE II  
COMPARISON OF AVERAGE PROCESSING TIME

Method	Processing Time [sec]
ICP	2.85
ICP with ANN	0.23
ICP with ANN & Edge Detection	0.028

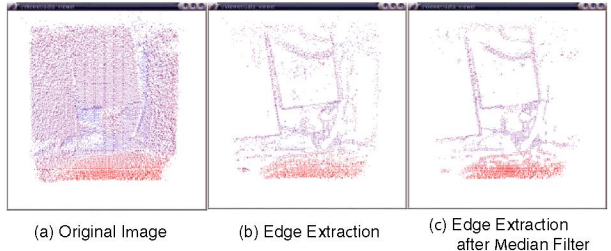


Fig. 6. Edge Extraction from Distance Image

The authors modified the step 1 for increasing its process speed and step 2 for increasing its robustness respectively. Details of these modifications are described in Sec. IV-B and Sec. IV-C.

##### B. Speedup of ICP Process

For speedup of ICP process, it is necessary to improve the corresponding point search process and to decrease iteration number of ICP. The authors reduced the processing time by modifying it as follows:

###### 1) Modification of Corresponding Point Search

The matching time can be decreased by reducing the number of scan points and changing the search algorithm. Concretely, points on edge were used for the motion estimation. The edge was extracted from gray image  $\mathbf{G}_t$ . Prewitt operator was used for the edge detection (Eq. (2)).

$$\begin{bmatrix} -1 & 0 & 1 \\ -1 & 0 & 1 \\ -1 & 0 & 1 \end{bmatrix}, \begin{bmatrix} -1 & -1 & -1 \\ 0 & 0 & 0 \\ 1 & 1 & 1 \end{bmatrix} \quad (2)$$

Median filter was applied to the gray image  $\mathbf{G}_t$  for noise reduction before the edge detection. Table III shows a result of position estimation. Accuracy of edge based matching is better than one of all point based matching. Details will be explained later.

ANN is used as search algorithm instead of kd-tree. Klurt et al. proposed the speedup of ICP using ANN [9]. Table II illustrates the average processing time of four steps (one iteration) in each ICP algorithm. The proposed method with edge detection and ANN can shorten processing time to 0.028[sec]. The processing time is 100 times as fast as normal one.

###### 2) Applying Initial Motion

For speedup of ICP process, it is necessary to reduce its iteration number. However, data thinning increases

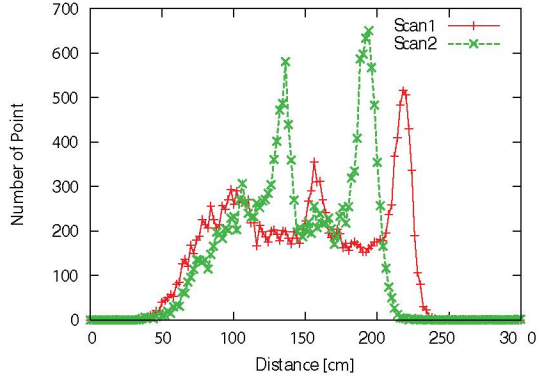


Fig. 7. Experiment of Distribution of Distance Data Points

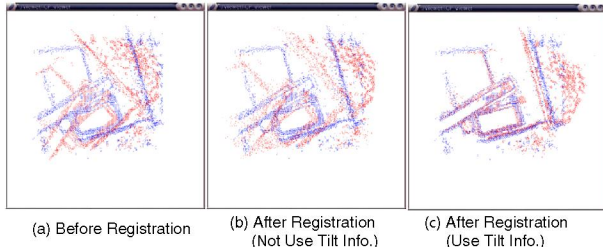


Fig. 8. Registration Experiment

iteration number of ICP process because estimated motion decreases in one iteration. Applying initial motion can reduce the iteration number in such situation. The initial motion was estimated from 3D camera data and accelerometer.

Initial translations along Z axis and X axis were calculated from the distribution of 3D camera data. Figure 7 shows the distributions of scan data's z which were measured at different viewpoint. The distribution shifts following the robot movement. However, this estimation is not suitable when the robot's rotation is large. The estimated initial translation was not used when the initial translation was larger than a threshold  $T_{x\text{ thresh}}, T_{z\text{ thresh}}$ .

Roll  $\phi$  and pitch  $\theta$  were applied to scan data when rotation was large. Figure 8 illustrates results of the matching method with initial motion estimation and without it. Applying initial rotation, the matching result became well as you can see.

### C. Elimination of Mismatched Point Pair

For accurate motion estimation, we should eliminate mismatched pair from the matched point list. The mismatch of point occurs by measurement error and change of visible area due to camera's narrow view angle. For accurate motion estimation, the authors eliminate the mismatched pair by following rules.

#### 1) Choice of Search Area Parameter $D_{max}$

The user can specified  $D_{max}$  which specifies an area for

the corresponding point search. Large  $D_{max}$  is better than small one when the motion between  $\mathbf{P}_{t-1}$  and  $\mathbf{P}_t$  is large. However, small  $D_{max}$  is better than large one for estimation of precise motion. Zhang proposed the decision rule of  $D_{max}$  for fast and accurate estimation [10]. The authors modified its parameters for our method. The  $D_{max}$  was changed by following rules:

$$\begin{aligned} \text{if } (\bar{d} < D/3) \quad D_{max} &= \bar{d} + 6\sigma_d; \\ \text{else if } (\bar{d} < D/2) \quad D_{max} &= \bar{d} + 4\sigma_d; \\ \text{else if } (\bar{d} < D) \quad D_{max} &= \bar{d} + 2\sigma_d; \\ \text{else} \quad D_{max} &= \bar{d}; \end{aligned}$$

$\bar{d}, \sigma_d, D$  represent mean of distance  $d$  between matched pair, standard deviation of  $d$  and  $D_{max}$  used in previous iteration respectively. Coefficient of  $\sigma_d$  were decided empirically.

#### 2) Angle between Matched Points

Direction of the matched points ( $\mathbf{x}, \mathbf{y}$ ) face same direction when the match is correct. Direction of each point  $\mathbf{x}, \mathbf{y}$  was calculated from adjoining points in  $\mathbf{P}_{t-1}, \mathbf{P}_t$  respectively. Validation of the point pair was checked by inner product of its direction. The pair is eliminated from the matched point list when the angle of inner product was larger than a threshold.

### D. Analysis of Accuracy

To analyze the accuracy of the proposed matching method, we compared the estimated robot position  $\mathbf{M}_t$  by our method with its true position  $\hat{\mathbf{M}}_t$ . In addition, we compared  $\mathbf{M}_t$  with the estimated robot position by ICP with ANN  $\mathbf{M}'_t$  [9]. The true motion  $\hat{\mathbf{M}}_t$  was measured by a motion capture whose accuracy was under 1 [cm]. We collected scan data which corresponded to translation along X and Z and rotation around X (Pitch), Y (Roll) and Z (Yaw) respectively. During the collection of these scan data, the robot moved 50 [cm] along X in 10 [cm/sec], 110 [cm] along Z in 20 [cm/sec], 22 [deg] around X in 5 [deg/sec], 25 [deg] around Y in 5 [deg/sec], and 45 [deg] around Z 5 [deg/sec]. The analysis was done for these five robot motions individually.

Figure 9 illustrates a graph of  $\hat{\mathbf{M}}_t$ ,  $\mathbf{M}'_t$  and  $\mathbf{M}_t$  in roll motion. In Fig. 9, x, pitch, yaw values also change according to roll change because snake-like robot consists of 3 bodies and two joints. Each motion was realized combination of some primitive motions. Therefore, all values change in translation along x, roll motion, pitch motion and yaw motion.

Table III shows average error between  $\hat{\mathbf{M}}_t$  and  $\mathbf{M}_t$  for the five motion, and average processing time. In Tab. III, accuracy of the modified ICP is better than one of ICP with ANN, except scan data of pitch. However, error of the modified ICP is  $-4.91[\text{cm}]$  as translation and  $3.39[\text{degree}]$  as rotation in the pitch motion. This error is not large. Moreover, in Tab. III, average z error of the modified ICP  $\bar{d}_z$  is  $-17.19[\text{cm}]$  when the robot moves 110 [cm] along z axis. Average error of x value is  $-7.78[\text{cm}]$  in the translation

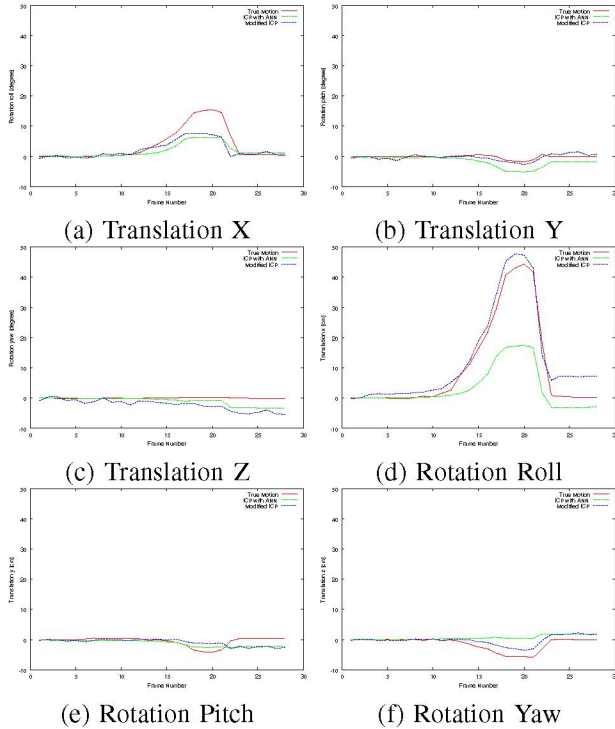


Fig. 9. Estimation Result for Roll Motion

motion along z. Estimation error of translation is between 15% and 17 %. Similarly, rotation is between 1 % and 15 %.

ThinkPad T42p was used for this calculation (Tab. IV). The processing time of modified ICP was good enough to estimate robot motion at 4 [fps].

## V. EXPERIMENT OF 3D MAP CONSTRUCTION

3D map construction was carried out in two different indoor environment. These map construction was done in offline. One is passage in the author's laboratory. The other is collapsed house simulation facility. The former environment is flat floor without any step. The latter one is not flat floor.

### A. System Construction

In this research, the authors used "IRS Souryu" developed by Tokyo Institute of Technology and IRS as mobile robot (Fig. 1). The robot moved at 44 [cm/sec] and 9 [deg/sec] as maximum. The authors provided it with 3D camera (CSEM Swiss Ranger2), laptop PC (VAIO typeU) and 3 DOF accelerometer (Crossbow CXL04LP3). Figure 10 illustrates its system construction. The 3D camera can measure 3D shape  $P_t$  and its texture  $G_t$ . Details of the sensor is explained in Sec. III. The robot's posture (Roll  $\phi$  and Pitch  $\theta$ ) is calculated from the accelerometer.

This system is constructed as a client server system. The client is the small-sized laptop PC which gathers measurement data from these sensors on the robot. The sever is

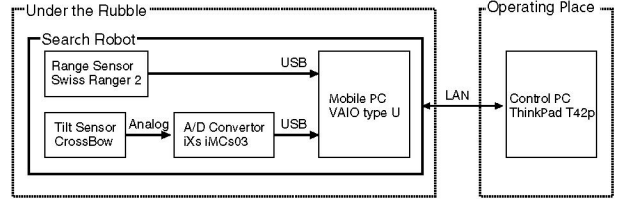


Fig. 10. System Architecture

TABLE IV  
PERFORMANCE OF COMPUTER

Item	Mobile PC	Operator's PC
Model	Sony Vaio VGN-U71P	IBM ThinkPad T42p
CPU	Intel PentiumM 1.10 GHz	Intel PentiumM 2.10 GHz
Memory	512 MB	2 GB

the laptop PC used for map construction and display. Table IV shows these laptop PCs' specification. LAN was used for connecting the client with sever. Measurement data are translated to operator's laptop PC via LAN. To apply a client server framework to the map construction system, we can equip any robot with it easily.

### B. Experiment at Passage in Laboratory

Robot moved along a trajectory in Fig. 11 in 15[cm/sec]. Distance of the trajectory was approximate 6.5 [m]. 3D data were measured in 4 [fps]. Figure 11 shows the constructed 3D map and the estimated trajectory. This map is represented in voxel whose size is 2 [cm], and color is painted from gray image  $G_t$ . Grid scale is 20 [cm]. The robot trajectory was estimated on the flat floor. We can recognize boxes and table on the floor in the constructed 3D map in Fig. 11. In other experiment, the estimated robot motion  $t_t$  was approximate 270 [cm] when the robot moved 300 [cm] along a straight line. Its error was 10 [%]. 3D map and robot trajectory was obtained by using the proposed method.

### C. Experiment in Collapsed House Simulation Facility

Collapsed House Simulation Facility is a test field for evaluation of rescue robots and tools. Figure 12 illustrates the test field and the obtained 3D map and robot trajectory. Grid size is 20 [cm].

The estimated robot trajectory was similar to real one. However, error of yaw rotation increased at first right turn from start point. The yaw rotation was not estimated by internal sensor in our approach. Therefore, error of yaw rotation increased when the robot's yaw rotation was large. The authors think that the use of gyro can solve this problem.

As you can see, wood pole on the ground near the first right turning point and white wood plate can be recognized in the constructed 3D map. However, visible area of the reconstructed 3D map was narrow. The 3D camera was narrow view angle and could not measure near distance. In

TABLE III  
COMPARISON OF ESTIMATION ACCURACY AND AVERAGE PROCESSING TIME

	Rotation Roll (45[deg]) ( $\bar{d}_x, \bar{d}_y, \bar{d}_z$ ) [cm] ( $\bar{d}_{roll}, \bar{d}_{pitch}, \bar{d}_{yaw}$ ) [deg]	Rotation Pitch (22[deg]) ( $\bar{d}_x, \bar{d}_y, \bar{d}_z$ ) [cm] ( $\bar{d}_{roll}, \bar{d}_{pitch}, \bar{d}_{yaw}$ ) [deg]	Rotation Yaw (25[deg]) ( $\bar{d}_x, \bar{d}_y, \bar{d}_z$ ) [cm] ( $\bar{d}_{roll}, \bar{d}_{pitch}, \bar{d}_{yaw}$ ) [deg]
ICP with ANN	(-1.80, -1.48, -1.07) (-6.72, -0.63, 1.90)	(-1.57, 1.14, -1.21) (-2.28, -2.27, -0.70)	(9.35, -0.14, 1.43) (-1.75, -0.02, -7.32)
Modified ICP	(-1.45, -0.14, -2.17) (2.66, -0.38, 1.10)	(-1.38, -4.91, 2.39) (-0.37, 3.39, -0.13)	(1.71, 1.76, 2.26) (-0.81, 0.87, 0.23)
	Translation X (50[cm]) ( $\bar{d}_x, \bar{d}_y, \bar{d}_z$ ) [cm] ( $\bar{d}_{roll}, \bar{d}_{pitch}, \bar{d}_{yaw}$ ) [deg]	Translation Z (110[cm]) ( $\bar{d}_x, \bar{d}_y, \bar{d}_z$ ) [cm] ( $\bar{d}_{roll}, \bar{d}_{pitch}, \bar{d}_{yaw}$ ) [deg]	Matching Time ( $t_{max}, t_{min}$ ) [sec]
ICP with ANN	(-24.26, 0.91, 1.12) (3.21, -0.08, -0.47)	(2.401, -6.76, -44.64) (1.20, -4.29, 0.47)	(0.44, 1.58, 0.14)
Modified ICP	(-7.78, 0.71, -0.42) (0.59, 0.35, -2.53)	(5.17, -3.84, -17.19) (1.31, -3.87, 1.33)	(0.13, 0.35, 0.03)

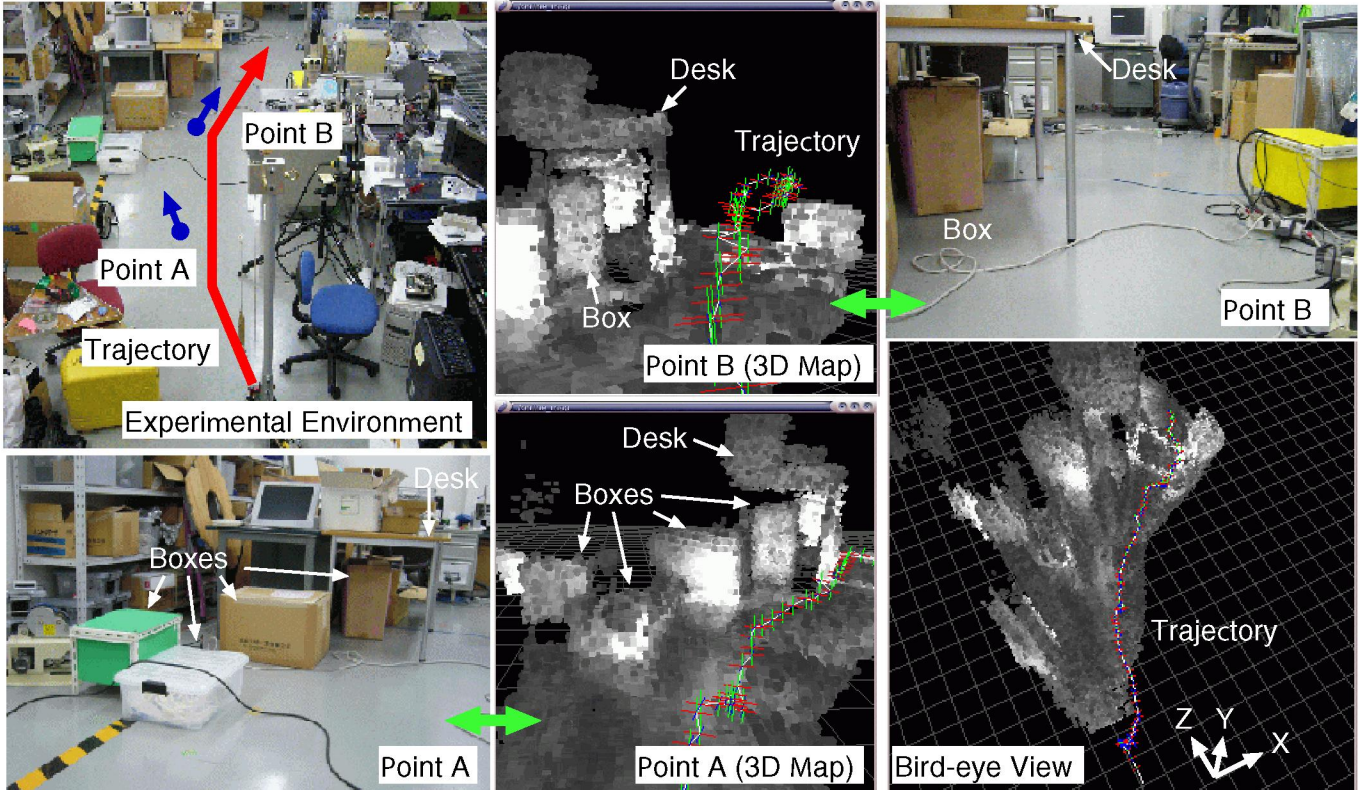


Fig. 11. Snapshots of Experimental Environment and Constructed 3D Map

the rubble, it is hard for the robot to face the 3D camera at all direction. The authors think that it is necessary for the 3D camera to measure short range and wide view angle for 3D map construction in the rubble environment.

## VI. CONCLUSION

The authors proposed real-time SLAM based on 3D scan match. 3D camera was used for measurement of 3D shape and its texture in real-time. 3D map and robot trajectory were estimated by combining these 3D scan data. ICP algorithm was used for the matching method. As 3D map must be constructed in real-time, the authors modified ICP algorithm as fast and robust one. The processing time of ICP algorithm developed by the authors was 100 times as fast as normal one. The accuracy of our method was higher than that of normal ICP algorithm on the whole. 3D map construction was

successful on flat floor in laboratory. However, in experiment in collapsed house simulation facility, rubble environment arose two problems: large error of yaw rotation and narrow visible area in 3D map. The authors think that the use of gyro can solve the problem of yaw rotation. To solve the problem of narrow visible area, it is necessary for the 3D camera to measure short range and wide view angle.

## ACKNOWLEDGMENTS

This research has been partially supported by MEXT Grant-in-Aid for Young Scientists (B) under contact numbers 17700193, 2005, and has been performed as a part of Special Project for Earthquake Disaster Mitigation in Urban Areas (in cooperation with International Rescue System Institute (IRS) and National Research Institute for Earth Science and Disaster Prevention (NIED)).

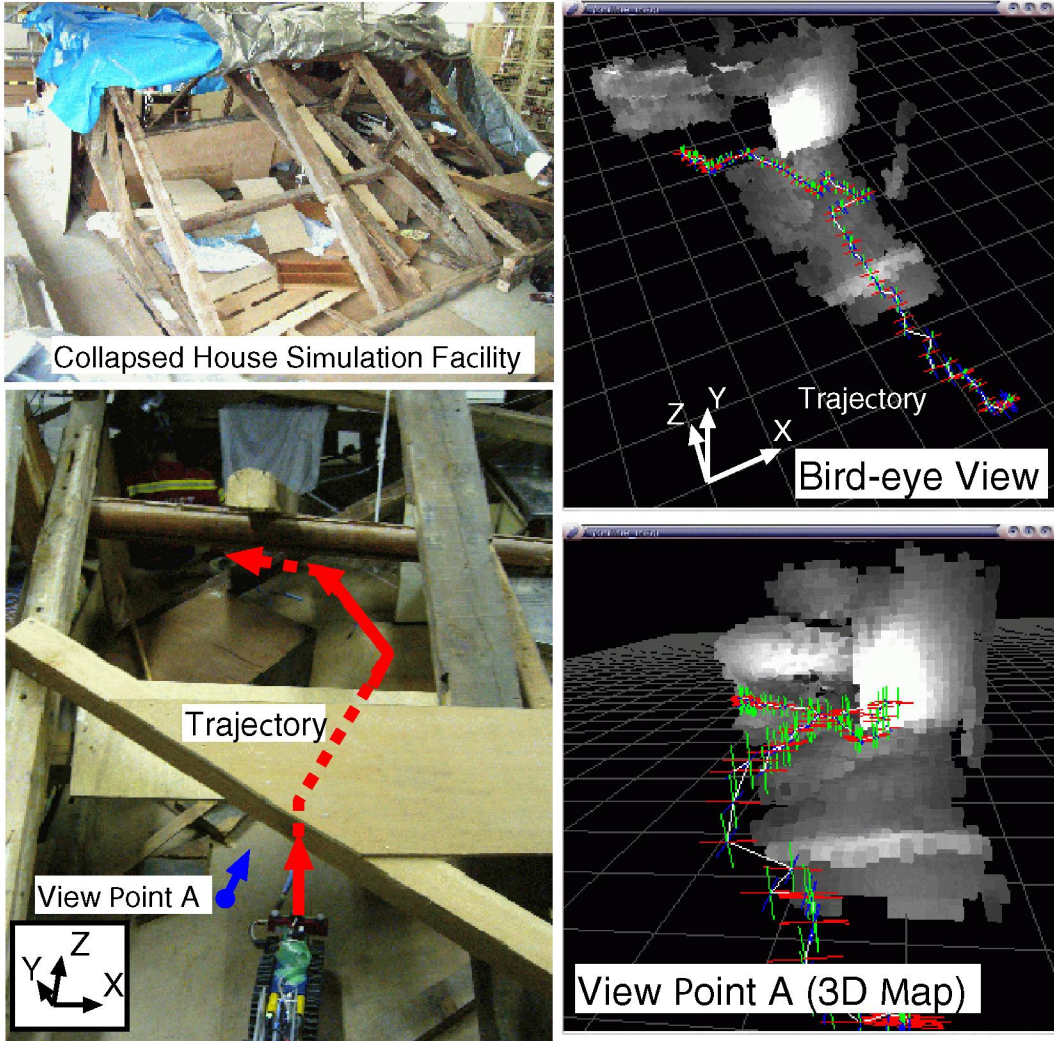


Fig. 12. Snapshots of Collapsed House Environment and Constructed 3D Map

## REFERENCES

- [1] J. Leonard, J.D. Tardos, S. Thrun and H. Choset eds., "Workshop Notes of the ICRA Workshop on Concurrent Mapping and Localization for Autonomous Mobile Robots," ICRA, 2002.
- [2] S. Thrun, M. Diel, D. Hahnel, "Scan Alignment and 3-D Surface Modeling with a Helicopter Platform," The 4th International Conference on Field and Service Robotics, 2003.
- [3] H. Baltzakis, P. Trahanias, "Closing Multiple Loops while Mapping Features in Cyclic Environments," Int. Conf. on Intelligent Robots and Systems, pp. 717–pp. 722, 2003.
- [4] C. C. Wang, C. Thorpe, S. Thrun, "Online Simultaneous Localization And Mapping with Detection And Tracking of Moving Objects: Theory and Results from a Ground Vehicle i Crowd Urban Areas," Proc. of ICRA, 2003.
- [5] D. Hähnel, R. Triebet, W. Burgard, S. Thrun, "Map Building with Mobile Robots in Dynamic Environments," Proc. of ICRA, 2003.
- [6] J. Guivant, E. Bebot, "Improving Computational and Memory Requirements of Simultaneous Localization and Map Building Algorithms," Proc. of IEEE Int'l Conference on Robotics and Automation, pp. 2731–pp. 2736, 2002.
- [7] K. Ohno, T. Tsubouchi and S. Yuta, "Outdoor Map Building Based on Odometry and RTK-GPS Positioning Fusion," Proc. of ICRA, pp. 687–pp. 690, 2004.
- [8] H. Ishida, K. Nagatani and Y. Tanaka, "Three-Dimensional Localization and Mapping for a Crawler-type Mobile Robot in an Occluded Area Using the Scan Matching Method," Proc. of IEEE/RSJ Int. Conf. on Intelligent Robots and Systems, pp. 449–pp. 454, 2004.
- [9] A. Nuchter, H. Surmann, K. Lingemann, J. Hertzberg and S. Thrun, "6D SLAM with an Application in Autonomous Mine Mapping," Proc. of ICRA 2004, pp. – pp. ,2004.
- [10] Z. Zhang, "Iterative Point Matching for Registration of Free-Form Curves," INRIA Rapports de Recherche, No. 1658, Programme 4, Robotique, Image et Vision, 1992.
- [11] M. W. Walker, L. Shao and R. A. Volz, "Estimating 3-D location parameters using dual number quaternions," CVGIP:Image Understanding, vol. 54, pp. 358–pp. 367, November 1991.
- [12] J.W. Weingarten, G. Gruener and R. Siegwart, "A State-of-the-Art 3D Sensor for Robot Navigation," Proc. of IEEE/RSJ Int. Conf. on Intelligent Robots and Systems, pp. 2155– 2160, 2004.
- [13] K. Ohnop and S. Tadokoro, "Dense 3D Map Building based on LRF data and Color Image Fusion," Proc. of IEEE/RSJ Int. Conf. on Intelligent Robots and Systems, pp. 1774– 1779, 2005.